

## ADHESIVELY BONDED AND HYBRID CLT PANEL-TO-PANEL JOINTS

Alicja Pace<sup>1</sup>, Houman Ganjali<sup>2</sup>, Lei Zhang<sup>3</sup>, Hercend Mpidi Bitu<sup>4</sup>, Thomas Tannert<sup>5</sup>

**ABSTRACT:** Cross-laminated timber (CLT) panels are increasingly being used in floor construction with the individual panels often connected with self-tapping screws (STS) through surface spline, half-lap, and butt joints. An alternative solution is provided by using the TS3 technology which connects butt joints through adhesives and creates a near-rigid connection, enabling the utilization of the two-way resistance of CLT panels. However, TS3 joints fail in a brittle manner. To address this issue, in this study, the mechanical properties of screw, TS3, and hybrid TS3-screw connections between CLT in the major and minor strength directions were investigated using out-of-plane 3-point and 4-point bending tests. The tests showed brittle failure for TS3 joints and ductile failure for STS joints, while the hybrid joints had similar stiffness as the TS3 joints.

**KEYWORDS:** cross-laminated timber, rotational stiffness, self-tapping screws, spline connection

### 1 – INTRODUCTION

There is a need for research to develop novel and value-added applications for wood to reduce the carbon footprint of buildings. Cross-laminated timber (CLT) provides many benefits compared to light-frame wood, such as a high-level of prefabrication and fast erection. When used as a floor diaphragm, CLT panels resist out-of-plane gravity loads and in-plane lateral loads [1].

To successfully build CLT floors, connections between individual panels need to be designed for appropriate strength, stiffness, and ductility. Traditional panel-to-panel connections employ dowel-type fasteners such as self-tapping screws (STS) to transfer in-plane shear force [2]. The desire for open space and clear storey height favours the use of flat-plate systems where CLT panels are point-supported by columns and span two ways. In such systems, the performance of connections is critical to engage two-way behaviour. However, screw connections have limited moment capacity under out-of-plane loads. As a result, CLT panels are often designed as a one-way system.

The TS3 adhesive bonding technology, which provides near-rigid connections, is an alternative [3] to mechanical fasteners. However, the ductility of CLT diaphragms relies on the connections, and engineers are reluctant to use pure adhesive connections due to the brittle failure modes.

The combination of TS3 and STS offers a possible solution for achieving both high stiffness and high ductility. In such hybrid joints [4], the adhesive provides near-rigid stiffness under service loads, while screws act as a backup system for

a failing bond and can be designed for failure loads only. Hybrid TS3 and STS joints have been applied to a prototype case study building, ‘oN5’ in Vancouver [5].

### 2 – MATERIALS AND METHODS

#### 2.1 TEST SERIES OVERVIEW

Three joint configurations were fabricated and subsequently tested at the Wood Innovation Research Lab in Prince George, British Columbia: Type (A) – TS3 adhesive system; type (S) – STS installed at 45 degrees to the surface; and type (AS) – a hybrid solution combining the TS3 with STS.

Two test methods were adopted: (B) four-point bending tests with the joint in the shear-free zone and largest bending moment; and (S) three-point bending tests with the joint exposed to the maximum shear-force and reduced bending moment. Two CLT lay-ups (5-ply and 7-ply) were used with joints created in the CLT panel major and minor directions (y and i). It should be noted that the majority of tests were conducted on joints in the minor strength axis of CLT panels, since the limited width of CLT panels always requires joints in this orientation.

An overview of the test series is shown in Table 1. The series label consists of test method, CLT layout, panel orientation and joint detail, e.g. the label ‘B-7i-AS (12)’ stands for a 7-ply panel connected in the minor-strength-axis with a hybrid joint combining the TS3 technology with 12 STS, tested under four-point bending. Each test series had six replicates, for a total of 126 tests.

<sup>1</sup> Alicja Pace, School of Engineering, University of Northern British Columbia, Prince George, Canada, Alicja.Pace@unbc.ca

<sup>2</sup> Houman Ganjali, School of Engineering, University of Northern British Columbia, Prince George, Canada, ganjali@unbc.ca

<sup>3</sup> Lei Zhang, School of Engineering, University of Northern British Columbia, Prince George, Canada, lei.zhang@unbc.ca

<sup>4</sup> Hercend Mpidi Bitu, Timber Engineering Inc. Vancouver, Canada, hercend.mpidibitu@timberengineering.ca

<sup>5</sup> Thomas Tannert, School of Engineering, University of Northern British Columbia, Prince George, Canada, thomas.tannert@unbc.ca

Table 1: Test series overview

| Test series | Method          | Layup       | Axis        | Joint type  |        |
|-------------|-----------------|-------------|-------------|-------------|--------|
| B-5y-A      | 4-point bending | 5-ply       | Major       | TS3         |        |
| B-5y-S(6)   |                 |             |             | 6×STS       |        |
| B-5y-S(18)  |                 |             |             | 18×STS      |        |
| B-5y-AS(6)  |                 |             | TS3+ 6×STS  |             |        |
| B-5y-AS(18) |                 |             | TS3+ 18×STS |             |        |
| B-5i-A      |                 |             | Minor       | STS         |        |
| B-5i-A2     |                 | TS3         |             |             |        |
| B-5i-S      |                 | TS3         |             |             |        |
| B-5i-AS(12) |                 | 7-ply       | Minor       | TS3+ 12×STS |        |
| B-7i-S      |                 |             |             | 12×STS      |        |
| B-7i-A      |                 |             |             | TS3         |        |
| B-7i-AS(12) |                 |             | TS3+ 12×STS |             |        |
| S-5y-S(18)  | 3-point bending |             | 5-ply       | Major       | 18×STS |
| S-5y-A      |                 |             |             |             | TS3    |
| S-5y-AS(18) |                 | TS3+ 18×STS |             |             |        |
| S-5i-S(12)  |                 | Minor       |             | 12×STS      |        |
| S-5i-A      |                 |             |             | TS3         |        |
| S-5i-AS(12) |                 |             |             | TS3+ 12×STS |        |
| S-7i-S(12)  |                 | 7-ply       | Minor       | 12×STS      |        |
| S-7i-A      |                 |             |             | TS3         |        |
| S-7i-AS(12) |                 |             |             | TS3+ 12×STS |        |

## 2.2 MATERIALS

Two CLT lay-ups were used: 5-ply (175 mm thick) and 7-ply (245 mm thick) grade V2 manufactured in accordance with ANSI/APA PRG 320 [6]. The specimens were 550 mm wide. The moisture content at the time of testing, determined using a resistance moisture meter, ranged from 11% to 12%.

Purbond PTS CR192, a 2K PU adhesive, developed for the purpose of bonding wood elements, including at the end-grain, and produced without the incorporation of solvents or formaldehyde, was used to connect the panels [7].

The STS were Ø8 mm Klimas WKFC fully-threaded cylindrical head screws, made of carbon steel with a tensile capacity of 25 kN [8]. Two lengths of screws were used: 220 mm for the 5-ply panels and 300 mm for the 7-ply panels, both installed at 45° to the surface of CLT. Different screw spacings were adopted based on the number of installed STS.

## 2.3 JOINT ASSEMBLY

For the (A) and (AS) test series, one end of each CLT segment was cut to create a fresh surface which was coated with CR192 pretreatment [7], as shown in Fig. 1a. The joints were assembled within the next 2 hours. The segments were held in position with a 5 mm spacer to maintain a constant gap. This gap was sealed with watertight tape acted as a casting mold. Then, the adhesive was injected into the joint from a diagonal hole, as shown in Fig. 1b. The glue injection continued until no air pockets remained. The curing time prior to testing was three days for the specimens jointed in the major-strength direction and B-5i-A and then increased to seven days for the rest of the test specimens.

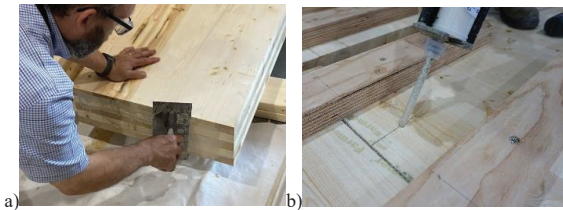


Figure 1. Preparation: a) Surface pre-treatment; b) Adhesive injection

## 2.4 BENDING TESTS

In the four-point bending tests, the load was applied to the third points of the specimens with the joint at the mid-span which was shear-free and had maximum bending moment, as shown in Fig. 2a. The distance between the third points was 1100 mm for the major strength axis tests and 660 mm for the minor-strength-axis tests; the only exception was B-5i-A which was 1100 mm in the minor strength direction. The span-to-depth ratio of the series was designed with reference to PRG-320 [6] as 18.8 for major strength axis tests and B-5i-A, and 11.3 and 8.0 for the 5- and 7-ply minor strength axis tests, respectively.

The three-point bending test setup is shown in Fig. 2b. The distance between the supports and the mid-point was 300 mm. The joint was at the quarter span, while the load was applied at the mid-span. In this manner, the connection was subjected to the maximum shear force combined with 50% of the maximum bending moment.

The tests were conducted in accordance with ISO 6891 [9] with a 500 kN hydraulic actuator at a constant rate of loading of 10 mm/min. The specimens were line-supported along width on steel rollers at both ends. The vertical displacement of the underside of the specimens at mid-span as well as the gap opening at the bottom of joints was measured using string pots.



Figure 2. Test setup: a) four-point bending; b) three-point bending.

## 2.6 ANALYSES

Modulus of rupture  $S_R$  (as a proxy for maximum bending stress in TS3 and hybrid series), apparent bending stiffness  $EI_{app}$  (which includes the shear deformation), maximum shear stress  $\tau_{max}$ , and the maximum bending moment at the joint  $M_{max}$ , were calculated. The serviceability rotational stiffness ( $C_\Phi$ ) was determined based on the slope of the moment-rotation curve in the range of 10% to 40% of the peak load. Ductility  $\mu$  was determined based on the ratio of ultimate displacement  $d_{ult}$  to yield displacement  $d_Y$  as per ISO/TR 21141 [10], with  $d_{ult}$  being the deflection at failure. Ductility was evaluated using the scale proposed by Smith et al. [11] with brittle ( $\mu \leq 2$ ), low ductility ( $2 \leq \mu \leq 4$ ), moderate ductility ( $4 \leq \mu \leq 6$ ) and high ductility ( $\mu > 6$ ).

## 3 – RESULTS AND DISCUSSION

### 3.1 FOUR-POINT BENDING TESTS

The load-displacement curves from the four-point bending are illustrated in Fig. 3. All adhesive and hybrid joints exhibited quasi-linear behavior up to the peak load. In the STS joints, stiffness slightly decreased while approaching load-carrying capacity. Beyond that point, a long plateau of constant residual strength was observed followed by a gradual drop of strength. In contrast, the TS3 and hybrid series exhibited no load-carrying capacity beyond the peak.

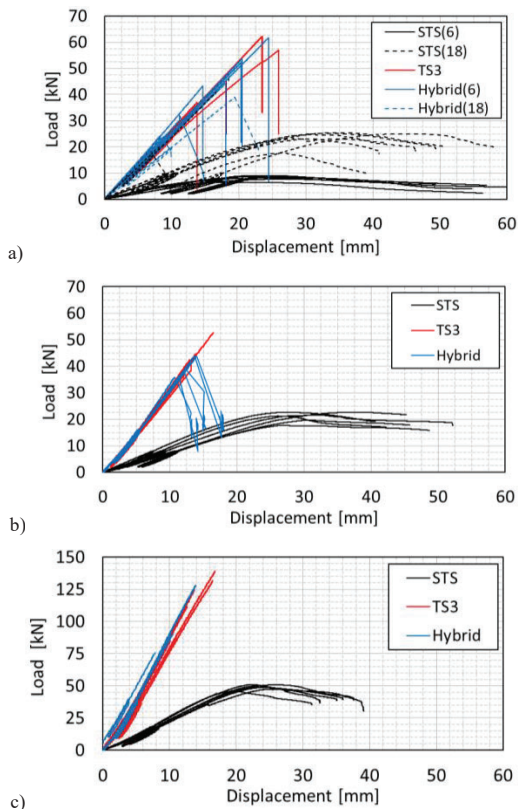


Figure 3. Four-point bending load-displacement: a) 5-ply major axis; b) 5-ply minor axis; c) 7-ply minor axis.

The failure modes of the specimens tested in four-point bending are illustrated in Fig. 4. STS joints exhibited a gap opening at the bottom of specimen and minor local crushing and splitting at the top of specimen (Fig. 4a); however, this damage did not result in global joint failure. B-5y-S(6) joints did not exhibit splitting at the top in the longitudinal layer due to the relatively low resistance of the 6 screws.

The TS3 joints exhibited a brittle bond-failure, see Fig. 4b and c, with fiber-rupture evident in the transverse layers where the side-grain was bonded with the adhesive; this failure was consistent across major- and minor-axis-oriented series as well as the 5- and 7-ply series.

The specimens with the hybrid joint also exhibited a brittle failure and the same fiber-rupture as in the TS3 joints (Fig. 4d and e). However, the STS preserved some structural integrity and prevented the joint from falling apart. Failure mechanisms of joints in the minor- and major-strength-axis oriented series having the same type of joint were the same.



Figure 4. Typical failure modes in four-point bending tests.

The bending moment capacity  $M_{max}$ , modulus of rupture  $S_R$ , apparent bending stiffness  $EI_{app}$ , and the rotational stiffness  $C_\varphi$ , as well as their coefficients of variation (CoV) from the four-point bending tests are summarized in Table 2.

In the major-strength-axis tests, the  $M_{max}$  and  $S_R$  of STS joints with 6 and 18 screws were 15% and 46% of the TS3 joints, respectively. The  $M_{max}$  of the 6- and 18-screw hybrid joints reached 89% and 65% of the TS3 joints, respectively. In the minor-strength-axis tests,  $M_{max}$  and  $S_R$  of the STS joints were 51% and 43% of the TS3 joints for 5-ply and 7-ply, respectively, whereas  $M_{max}$  of the hybrid joints reached 97% and 93% of the TS3 joints. In the hybrid joints, the adhesive bond acted as the primary resisting mechanism while the screws were intended to perform as secondary resisting mechanism after failure of the adhesive bond.

In the major-strength-axis,  $S_R$  of the TS3 joints was 10.5 MPa;  $S_R$  for the hybrid joints was 9.5 MPa and 6.8 MPa for the 6- and 18-screw specimens, respectively; and  $S_R$  for 6 and 18 screw joints was 1.6 MPa and 4.8 MPa, respectively. In CSA O86 [12], the specified bending strength of V2 grade CLT in the major strength direction is 11.8 MPa. The 5<sup>th</sup> percentile  $S_R$  value across the adhesive and hybrid joints, adjusted for standard load duration determined with the ASTM D2915 [13] parametric method, was 3.6 MPa, which was much lower than the specified bending strengths of V2 grade CLT [12]. It should be noted that two weak 18-STs hybrid joints resulted in the low 5<sup>th</sup> percentile values while these series had  $S_R$  of 8.9 MPa. To determine the characteristic bending strength, a larger sample size would be required.

In the minor strength direction,  $S_R$  of the TS3 joints averaged at 13.3 MPa for both 5- and 7-ply series;  $S_R$  for the STS 5- and 7-ply joints were 6.8 MPa and 5.7 MPa, respectively; and  $S_R$  for the hybrid 5- and 7-ply joints are 12.9 MPa and 12.3 MPa, respectively. In CSA O86 [12], the specified bending strength of V2 grade in the minor strength direction

is 7.0 MPa. The 5<sup>th</sup> percentile  $S_R$  value across the adhesive and hybrid series determined with ASTM D2915 [13] parametric method and adjusted for standard load duration was 6.9 MPa. This finding suggests that TS3 and hybrid joints reach a similar magnitude of out-of-plane bending resistance as the CLT panel in minor-strength-axis. The  $S_R$  of B-5i-A with a 3-day curing averaged at 10.9 MPa whereas the  $S_R$  of B-5i-A2 with a 7-day curing was 13.3 MPa.

The apparent bending stiffness  $EI_{app}$  of the 6- and 18- screw joints in the major-strength-axis reached an average of only 21% and 37%, respectively, of the TS3 joints (1,593 kNm<sup>2</sup>), while the hybrid joints reached 100% and 80%. The average  $EI_{app}$  of the adhesive and hybrid joints was roughly 80% the  $EI$  according to CSA O86 [12]. In the minor-strength axis,  $EI_{app}$  of the 12-STs joints was roughly one-third of the TS3 joints (B-5i-A2) at 423 kNm<sup>2</sup>, while the hybrid series had almost the same  $EI_{app}$  as B-5i-A2 TS3 joints. The average  $EI_{app}$  of the TS3 series in the minor strength direction was at a similar magnitude as the  $EI_{ef}$  according to CSA O86 [12] for the tested CLT layups and stress grades.

The rotational stiffness  $C_\varphi$  in the major-strength-axis was 7,299 kNmrad<sup>-1</sup> for the TS3 joints which is not significantly different from the 6- and 18-screw hybrid joints with roughly 6,800 kNmrad<sup>-1</sup> and 8,400 kNmrad<sup>-1</sup>, respectively.  $C_\varphi$  of the adhesive joints was 21 and 83 times of the 6- and 18-screw joints. In the minor-strength-axis series,  $C_\varphi$  of the 5-ply and 7-ply TS3 joints was 5,575 kNmrad<sup>-1</sup> and 24,207 kNmrad<sup>-1</sup>, respectively. The hybrid 5-ply and 7-ply joints exhibited rotational stiffness of 7,419 kNmrad<sup>-1</sup> and 23,668 kNmrad<sup>-1</sup>, respectively. It can be observed that major- and minor-strength-axis TS3 and hybrid joints having the same layup had similar rotational stiffness. In both directions, the rotational stiffness of TS3 and hybrid joints exceeded the threshold of 5,000 kNmrad<sup>-1</sup> reported in the literature [14-15], effectively creating a rigid connection.

Table 2: Results of four-point bending tests.

| Series      | $M_{max}$ | $S_R$ | CoV | $EI_{app}$          | CoV | $C_\varphi$             | CoV | $\mu$ |
|-------------|-----------|-------|-----|---------------------|-----|-------------------------|-----|-------|
|             | [kNm]     | [MPa] | [%] | [kNm <sup>2</sup> ] | [%] | [kNmrad <sup>-1</sup> ] | [%] | [-]   |
| B-5y-S(6)   | 4.4       | 1.6   | 10  | 342                 | 11  | 345                     | 13  | 3.6   |
| B-5y-S(18)  | 13.4      | 4.8   | 4   | 592                 | 20  | 881                     | 19  | 2.2   |
| B-5y-A      | 29.4      | 10.5  | 17  | 1593                | 4   | 7299                    | 11  | 1.0   |
| B-5y-AS(6)  | 26.3      | 9.4   | 20  | 1607                | 5   | 6797                    | 6   | 1.0   |
| B-5y-AS(18) | 19.2      | 6.8   | 29  | 1281                | 35  | 8379                    | 19  | 1.0   |
| B-5i-S(12)  | 6.9       | 6.8   | 8.3 | 119                 | 17  | 357                     | 13  | 2.6   |
| B-5i-A      | 11.0      | 10.9  | 22  | 565                 | 6   | 2583                    | 13  | 1.0   |
| B-5i-A2     | 13.4      | 13.3  | 19  | 423                 | 7   | 5575                    | 8   | 1.0   |
| B-5i-AS(12) | 13.0      | 12.9  | 8   | 413                 | 4   | 7419                    | 14  | 1.0   |
| B-7i-S(12)  | 16.1      | 5.7   | 4   | 376                 | 8   | 1002                    | 7   | 2.4   |
| B-7i-A      | 37.3      | 13.3  | 19  | 1127                | 7   | 24207                   | 8   | 1.0   |
| B-7i-AS(12) | 34.5      | 12.3  | 20  | 1213                | 10  | 23668                   | 17  | 1.0   |

### 3.3 THREE-POINT BENDING TESTS

The load-displacement curves from the three-point bending tests are shown in Fig. 5. In both strength axis orientations, adhesive and hybrid joints exhibited quasi-linear behavior up to peak load. The STS joints exhibited some residual deformation capacity beyond peak load when the screws started to withdraw. TS3 and hybrid joints did not show residual deformation capacity with the STS in the hybrid joints exhibiting minimal resistance after bond failure.

The typical failure modes are illustrated in Fig. 6. STS joints exhibited gap opening at the bottom face, combined with minor local crushing of the topmost CLT layer with some minor cracks, see Fig. 6a, and some splitting of the topmost and second topmost layer in major- and minor-strength-axis oriented series respectively; these local failures did not lead to any abrupt change in the load-carrying behavior.

Failure of the 5-ply TS3 joints was brittle accompanied by side grain fibre-rupture (Fig. 6b); however, no sign of wood fibre failure was observed where end-grain was bonded. One of the 7-ply TS3 joints had complete joint failure exhibiting the same side-grain rupture mode as the 5-ply joints, two had partial failure with extended cracks (Fig. 6c); and three specimens did not fail in the joint but in CLT rolling shear. In the 7-ply hybrid series, only one specimen partially failed in the joint while the rest exhibited CLT rolling shear failure. The hybrid major-strength-axis series experienced the same partial failure.

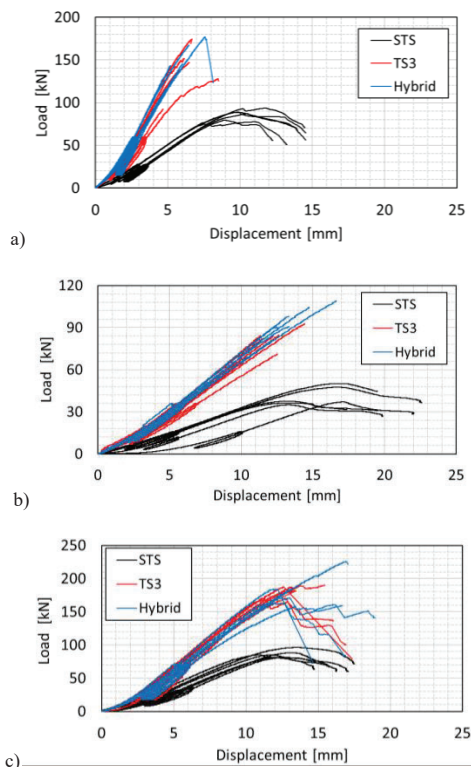


Figure 5. Three-point bending load-displacement: a) 5-ply major axis; b) 5-ply minor axis; c) 7-ply minor axis.

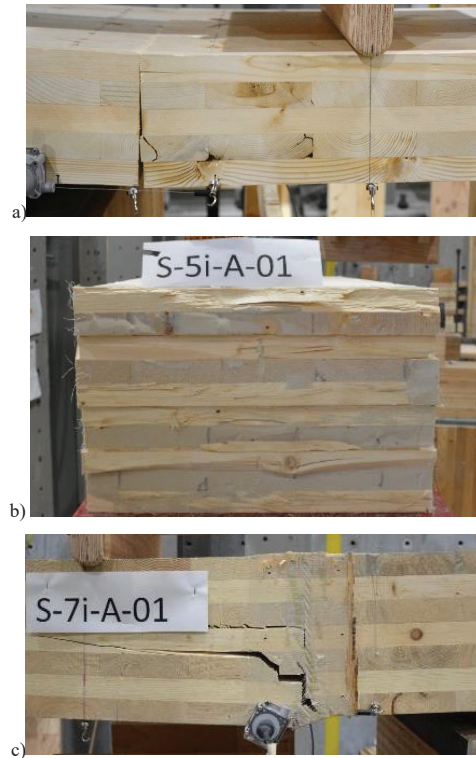


Figure 6. Typical failure modes in three-point bending tests.

The average values of maximum shear force  $F_{max}$ , bending moment capacity  $M_{max}$ , maximum shear stress  $\tau_{max}$ , rotational stiffness  $C_{\Phi}$ , and ductility  $\mu$  and their corresponding CoV, from the three-point bending tests are summarized in Table 3.

In the major-strength-axis, bending moment capacity of TS3 joints was 19.5 kNm, and for the hybrid joints the moment capacity was 22.4 kNm, while the STS joints, on average, reached 66% of the TS3 joints  $M_{max}$ . In minor-strength-axis,  $M_{max}$  of both 5-ply (13.9 kNm) and 7-ply (29.1 kNm) TS3 joints were almost twice that of STS joints; the 5-ply hybrid joints were 16% stronger than 5-ply TS3 joints. The minor-strength-axis 7-ply hybrid series reached almost the same  $M_{max}$  as the 7-ply TS3 despite having multiple specimens failing in rolling shear.

Maximum shear stresses  $\tau_{max}$  ranged from 1.0 MPa to 1.4 MP. Under the 3-point bending, due to the out of plane bending, the shear force caused perpendicular side-grain rupture. At 5<sup>th</sup> percentile level and adjusted for standard load duration these values ranged from 0.6-1.1 MPa which is higher than specified rolling shear strength of V2 stress grade CLT in CSA O86[12] but close to the rolling shear strength of Grade V2 CLT reported in the literature [16].

Rotational stiffness  $C_{\Phi}$  of the 5- and 7-ply-i TS3 joints was 7,355 kNmrad<sup>-1</sup> and 20,493 kNmrad<sup>-1</sup> respectively, up to 24

times the rotational stiffness of STS joints. The 5-ply-i hybrid joints reached a similar value of 7,139 kNmrad<sup>-1</sup>. Since only one 7-ply specimen from the hybrid series partially failed in the joint, the rotational stiffness value of this series was inconclusive. In the minor-strength-axis, the measured rotational stiffnesses from three-point bending tests were close to those from four-point bending tests, suggesting no impact from the concurrent shear force and bending moment in the three-point bending setup on  $C_{\Phi}$  of the joints.  $C_{\Phi}$  of TS3 and hybrid joints in the major-strength-axis was 7,573 kNmrad<sup>-1</sup> and 7,131 kNmrad<sup>-1</sup> respectively, almost 8 times the STS joints. The rotational stiffness of the minor- and major-strength-axis 5-ply TS3 and hybrid joint was within the same range under 3-point bending test, showing the same pattern as that of four-point bending tests where TS3 and hybrid joints of major- and minor-strength-axis series had similar rotational stiffnesses.

#### 4 – CONCLUSIONS

The structural performance of adhesively bonded, screwed and hybrid panel-to-panel CLT joints was assessed using out-of-plane four-point and three-point bending tests. The following conclusions can be drawn:

- Adhesively bonded and hybrid joints were effective in providing CLT panel continuity resulting in effective bending stiffness close to the values determined with CSA O86.
- Screwed joints in the minor- and major-strength-axis using 12 and 18 STS provided roughly 50% of the bending moment capacity of the adhesively bonded and hybrid joints.
- Although the STS in the hybrid joints did not prevent brittle failure, the screws showed the potential to provide a secondary load resistance mechanism in case of damage to the adhesive.

- The rotational stiffness provided by the TS3 and hybrid joints was well above the 5,000 kNmrad<sup>-1</sup>m<sup>-1</sup> threshold recommended in the literature to utilize two-way action in CLT floors, whereas STS solution alone could not provide sufficient rotational stiffness.
- In the minor-strength-axis, the 5<sup>th</sup> percentile modulus of rupture of 5- and 7-ply TS3 series adjusted for standard load duration was similar to the CSA O86 specified bending strength of V2 grade CLT.
- In the major-strength-axis, the 5<sup>th</sup> percentile modulus of rupture of the TS3 joints was much smaller than the CSA O86 specified bending strength for V2 grade CLT.
- Under three-point bending, some specimens with adhesive and hybrid joints experienced CLT rolling shear failure, indicating the adhesive bond was at least as strong as the CLT panels in rolling shear.

Drawing upon the findings of this research due to promising performance of adhesively bonded and hybrid joints, further experimental studies should aim to investigate their long-term performance, including that under changing environmental conditions.

#### ACKNOWLEDGEMENTS

The project was supported by the Natural Sciences and Engineering Research Council of Canada (NSERC) through an Alliance grant (ALLRP 580900-22) and a Mitacs Elevate grant (IT36800), both in collaboration between Timber Engineering Inc. and the University of Northern British Columbia. The support of following individuals is greatly appreciated: Maik Gehloff (WIRL lab lead), James Andal, Nathan Downie and Ryan Stern (technicians), Johannes Schneider (independent contractor), Sabarinath Sivakumar and Sanya Takur (Mitacs Globalink interns). The authors are thankful to Klimas and Timber Structures 3.0 AG for providing the self-tapping screws and the adhesive.

Table 3: Results of three-point bending tests.

| Series      | $F_{max}$ | $M_{max}$ | $\tau_{max}$ | CoV | $C_{\Phi}$              | CoV | $\mu$ |
|-------------|-----------|-----------|--------------|-----|-------------------------|-----|-------|
|             | [kN]      | [kNm]     | [MPa]        | [%] | [kNmrad <sup>-1</sup> ] | [%] | [-]   |
| S-5y-A      | 130.0     | 19.5      | 1.0          | 16  | 7,457                   | 20  | 1.0   |
| S-5y-S(18)  | 85.7      | 12.9      | [-]          | 6   | 982                     | 7   | 2.1   |
| S-5y-AS(18) | 149.3     | 22.4      | 1.2          | 14  | 8,360                   | 14  | 1.0   |
| S-5i-A      | 83.2      | 13.9      | 1.1          | 8   | 7,355                   | 16  | 1.0   |
| S-5i-S(12)  | 40.5      | 6.8       | [-]          | 15  | 312                     | 14  | 1.9   |
| S-5i-AS(12) | 96.8      | 16.1      | 1.3          | 10  | 7,140                   | 15  | 1.0   |
| S-7i-A      | 174.8     | 29.1      | 1.4          | 9   | 20,492                  | 6   | 1.0   |
| S-7i-S(12)  | 86.1      | 14.3      | [-]          | 6   | 938                     | 9   | 2.3   |
| S-7i-AS(12) | 178.4     | 29.7      | 1.4          | 12  | 18,880                  | 18  | 1.0   |

## REFERENCES

- [1] Karacabeyli E, Gagnon S. 2019. Cross-laminated timber (CLT) Handbook. FPIInnovations, Vancouver, Canada.
- [2] A. Hossain, M. Popovski, T. Tannert. "Cross-laminated timber connections assembled with a combination of screws in withdrawal and screws in shear." *Engineering Structures* 168 (2018), pp. 1–11.
- [3] S. Franke, S. Zöllig. 2020. "TS3 – A New Technology for Efficient Timber Structures." *Current Trends in Civil & Structural Engineering* 4.4 (2020), pp1-4.
- [4] T. Tannert, A. Gerber, T. Vallee. "Hybrid adhesively bonded timber-concrete-composite floors." *International Journal of Adhesion & Adhesives* 97 (2020), 102490.
- [5] L. Zhang, M. Muster, H. Mpidi Bitu, T. Tannert. "Robustness Of Adhesively Bonded Panel-To-Panel Connections in CLT Floors" In proc. World Conference on Timber Engineering, Oslo, Norway, 2023.
- [6] ANSI/APA PRG 320-2019 Standard for Performance-Rated Cross-Laminated Timber, APA – Engineered Wood Association, American National Standard Institute, New York, U. S., 20191983.
- [7] Z-9.1-917 Load-bearing glued cross-laminated timber elements "TS3-PTS elements" for floor and roof structures, Deutsches Institut für Bautechnik (DIBt), Berlin, 2024.
- [8] ETA-18/0817 Approval body for construction products and types of construction. Screws for use in timber constructions., KLIMAS screws, Mykanów, Poland, 2019.
- [9] ISO 6891, Timber structures — Joints made with mechanical fasteners — General principles for the determination of strength and deformation characteristics, 1983.
- [10] ISO/TR 21141:2022 Timber structures — Timber connections and assemblies — Determination of yield and ultimate characteristics and ductility from test data, International Organization for Standardization (ISO), Geneva, Switzerland, 2022.
- [11] I. Smith, A. Asiz, M. Snow, Y.H. Chui. "Possible Canadian/ISO approach to deriving design values from test data" In proc. CIB Working Commission W18 – Timber Structures, Karlsruhe, Germany, 2006.
- [12] CSA-O86 - Engineering Design in Wood, Canadian Standards Association, Mississauga, Canada, 2024.
- [13] ASTM D2915-17, Standard Practice for Sampling and Data-Analysis for Structural Wood and Wood Based Products, ASTM International, West Conshohocken, United States, 2017.
- [14] A. Hosseini, M. Shahnewaz, C. Dickof, Z. Jianhui, T. Tannert, "Moment connections in the minor strength axis of cross-laminated timber panels". In proc. 4th International Conference on New Horizons in Green Civil Engineering (NHICE-04), Victoria, Canada, 2024.
- [15] T. Stieb, B. Maurer, P. Dietsch, R. Maderebner. "Solutions for edge connections to build two-way spanning cross laminated timber slabs" In proc. World Conference on Timber Engineering, Oslo, Norway, 2023.
- [16] H. Ganjali, T. Tannert, M. Shahnewaz, C. Dickof, M. Popovski. "Punching-shear strength of point-supported CLT floor panels." In proc. International Network on Timber Engineering Research, Biel, Switzerland, 2023